KIT

Karlsruhe Institute of Technology

Optimization potentials of the transverse flux machine over the product life cycle

by Martin Schmid[1], Julian Schurr[2], Lukas Brandl[3], Ralf Sauerwald[3], Simon Knecht[4], Marcel Nöller[4], Yongxin Yu[5], Nejila Parspour[1], Frank Gauterin[5], Dagmar Goll[2], Hans-Christian Reuss[3], Albert Albers[4], Katharina Bause[4]

KIT SCIENTIFIC WORKING PAPERS   236

[1] Institute of Electrical Energy Conversion (IEW), University of Stuttgart
[2] Materials Research Institute (IMFAA), Aalen University
[3] Institute of Automotive Engineering (IFS), University of Stuttgart
[4] Institute of Product Engineering (IPEK), Karlsruhe Institute of Technology
[5] Institute of Vehicle System Technology (FAST), Karlsruhe Institute of Technology

Impressum

Karlsruher Institut für Technologie (KIT)
www.kit.edu

2023

ISSN: 2194-1629

Optimization potentials of the transverse flux machine over the product life cycle

M. Sc., Martin Schmid, University of Stuttgart, Stuttgart, Germany
M. Sc., Julian Schurr, Aalen University, Aalen, Germany
M. Sc., Lukas Brandl, University of Stuttgart, Stuttgart, Germany
M. Sc., Ralf Sauerwald, University of Stuttgart, Stuttgart, Germany
M. Sc., Simon Knecht, Karlsruhe Institute of Technology, Karlsruhe, Germany
M. Sc., Marcel Nöller, Karlsruhe Institute of Technology, Karlsruhe, Germany
M. Sc., Yongxin Yu, Karlsruhe Institute of Technology, Karlsruhe, Germany
Prof. Dr.-Ing., Nejila Parspour, University of Stuttgart, Stuttgart, Germany
Prof. Dr. rer. nat., Frank Gauterin, Karlsruhe Institute of Technology, Karlsruhe, Germany
Prof. Dr., Dagmar Goll, Aalen University, Aalen, Germany
Prof. Dr.-Ing., Hans-Christian Reuss, University of Stuttgart, Stuttgart, Germany
Prof. Dr.-Ing. Dr. h. c., Albert Albers, Karlsruhe Institute of Technology, Karlsruhe, Germany
Dipl.-Ing., Katharina Bause, Karlsruhe Institute of Technology, Karlsruhe, Germany

Abstract

This study focuses on improving the performance and reliability of a transverse flux machine (TFM) for automotive applications over the whole product life cycle. TFMs offer high torque density but present challenges in electromagnetic design, cooling, and vibration control. To address these issues, different measures like additive manufacturing, sensor integration, and optimization techniques are explored and evaluated. By incorporating sensors for real-time data collection during operation and integrating structural improvements during development, TFMs can achieve higher efficiency and reliability. This study gives an overview over several topics which have been researched in 2 projects, each of which consists of 3 participating institutions. It explores the integration of vibration sensors/actuators and temperature sensors. Additionally, additive manufacturing techniques are utilized for manufacturing of soft magnetic components to reduce eddy current losses and optimize the cooling. The findings demonstrate the potential of these approaches to enhance TFMs for automotive use, and further research is recommended to assess their durability and applicability under real-world conditions.

1 Introduction

Due to the electrification of the automotive drive systems, the use of electrical machines (EMs) is expected to increase rapidly. The usage of EMs in automotive use cases creates a high demand for reliability, performance, and efficiency. Reducing the various loss mechanisms and increasing the effective active volumes are important aspects to raise the performance and efficiency of EMs. Using transverse flux machines (TFMs), which are characterized by a high number of pole pairs leading to a high torque density, has a high potential to improve efficiency and performance. This high torque facilitates the removal of a currently required gearbox for machines operating at higher speeds and thus yields a better performance with respect to the assembly space. [1,2]

For this purpose, the structure of the TFM solves the trade-off between maximizing the copper and iron cross-sectional areas by means of decoupling the electric and magnetic cross sections. However, this decoupling leads to a required three-dimensional magnetic flux path and corresponding challenges for the electromagnetic design of the components. Also cooling and noise generation due to vibrations caused by the comparatively high cogging torque need to be taken into consideration. Compared to radial flux machines and their established conventional manufacturing processes, the increased manufacturing effort of TFMs due to the 3D magnetic flux can be significantly reduced by combining additive manufacturing processes with direct integration of functional components such as sensors and actuators.

Therefore, it becomes increasingly important to optimize the structure of the TFM and to directly measure a wide variety of variables in the TFM with newly integrated sensors. This contribution will explore the value added by a wider range of possible measures. From different sensor integrations to optimization aspects, additive manufacturing and cooling optimizations, various potentials are identified and discussed.

2 Product Life Cycle of Transverse Flux Machines

When incorporating sensors and actuators into an EM, it is paramount to maximize the usage of the collected data. Therefore, a framework was developed that allows sensor data to be collected and used holistically throughout the product life cycle and across product generations [3]. This framework draws from previous literature and thereby extends the ideas of Gausemeier et al. [4] as well as Sakao and Nordholm [5] who separate the lifecycle of a product

into four phases from Product design to End of Life and investigate the information flows between those phases. It also takes into account how specifications of e-machines are derived and which disciplines or roles of developers are involved in the exchange [6]. This knowledge is then applied to the TFM as an example product and shows the data exchange during the lifecycle but also between product generations.

A conventional design process uses analytical models and a loss calculation for pre-design, followed by electromagnetic design, which facilitates magnetic circuit models similar to electrical equivalent circuit models and finite element method (FEM) models. In thermal design, hybrid thermal networks with distributed heat sources are used. For the mechanical design, FEM models are relied upon to perform stress and vibration studies. Many of these models have a high number of input parameters, often taken from the literature or based on previous experience. Results from calculations can then themselves be input parameters for other models, so that errors can propagate and incorrect conclusions can be made. [7]

Thus, three types of data were identified with a potential benefit within one product lifecycle but also spanning multiple product generations [3, 4].

1. For electric modeling, the collection of further magnetic data on stray losses was identified as particularly relevant for the design process. These are difficult to estimate, but amount to up to 1 % of the output power [7]. This is not explored any further in this research.

2. Mechanical models of additively manufactured parts need to take new and challenging properties like porosities and changes in local densities into account, which were less of a concern for conventionally manufactured machines. Especially for NVH-modelling of the TFM, which, as mentioned before, still faces challenges in this area, this data could facilitate more precise models, better predictions and also inline quality assurance directly after additive manufacturing is complete.

3. Parameters for the thermal modeling of the individual components, e.g. the contact resistances, are dependent on many variables like contact pressure and surface qualities and therefore rely heavily on empirical data for very specific material combinations and operating conditions. Thermal simulations with wrong parameters may underestimate the prevailing temperatures due to insufficient knowledge of the resistances, which may contribute to an overestimation of the lifetime in operation. Better parametrized thermal models could help estimating the magnet temperature more precisely, preventing possible demagnetization and pushing the machine closer to its limits.

2.1 Mechanical Data Acquisition

For data acquisition for mechanical modelling, a vibration sensor / actuator (piezo patch) was selected. This sensor will be mounted on the spine of the TFM stator during or after manufacturing and can also be facilitated for active noise control during operation. Piezo elements are suitable for usage inside an EM due to properties such as a wide usable frequency range and a low installation space requirement. How to get the data required for Condition Monitoring (more specifically demagnetization) from simulation is now explained as an exemplary use case.

The whole procedure described in the following section about modeling the EM is similar to the procedure described in [8]. Since the used TFM has rotational symmetry, a single pole pair of the TFM can be used in simulation to reduce simulation time. A FEM model of a single pole pair was created in COMSOL (see **Figure 1**). Periodic boundary conditions were used in circumferential direction to create a full electrical phase of the TFM. The magnet in the center of the rotor segment is parametrized with different remanence flux densities (0.1 T, 0.4 T, 0.7 T, 1.0 T, 1.22 T). While 1.22 T represented the normal magnet, the other values represent different degrees of failure of the pole pair (from working to complete failure). Different angular positions of the rotor relative to the stator are simulated mimicking the passing of the faulty magnet over a stator tooth. The variation of magnetic flux on the tooth surface induces a force acting on the stator tooth. To reduce simulation time, the surface on the upper side of the stator tooth is split into discrete areas. The magnetic flux density is integrated in each area to receive an equivalent concentrated load for each area.
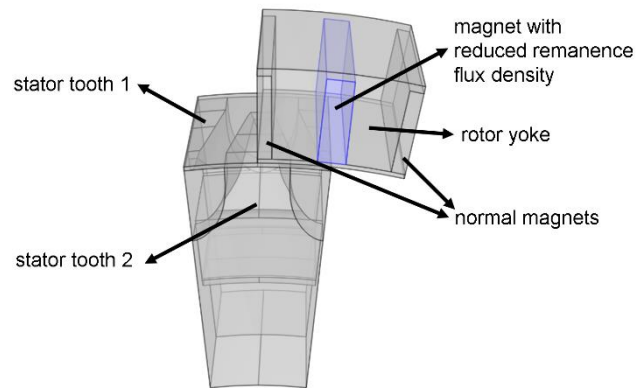
Figure 1: FEM model of a pole pair for simulating demagnetization

These concentrated forces are derived for all the different magnetic flux densities and for different angular positions of the rotor. Since only a partial rotation of the rotor is simulated (because rotational symmetry is used to reduce simulation time) and only one magnet is considered faulty, the simulated signals with different magnetic flux densities are extended with the signal from a run with the full magnetic flux density to receive the forces acting on a stator tooth for a full revolution of the rotor. To smooth the

transition between the signal with a faulty magnet and a normal magnet, a simple linear ramp is used to fade out one signal and fade in the other signal. By repeating the signals according to the number of stator teeth, a resulting radial force acting on the surface of a single tooth over a full revolution of the rotor can be received (see **Figure 2**). By assuming a constant angular velocity and dividing the angular positions by the angular velocity, these forces could be transferred from angular positions to time domain.
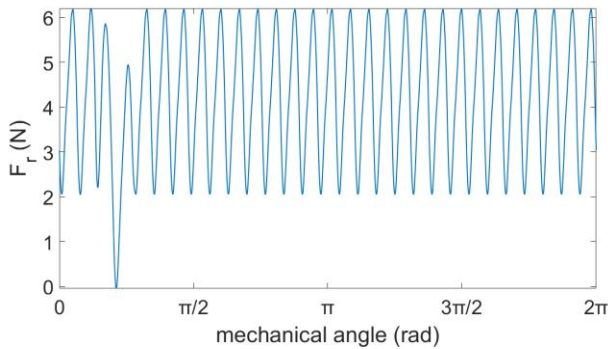
Figure 2: Radial force F_r acting on a single stator surface for a full revolution of the rotor

After the transformation to the frequency domain, the forces are used in a harmonic vibration analysis as excitation. For different stator teeth the excitation signal is shifted by a phase shift depending on the position of the stator tooth, to mimic the faulty magnet passing the different stator teeth one after another. As the whole TFM consists of three different electrical phases, the procedure described above with a faulty tooth is applied only to one electrical phase (see **Figure 3**). The other two phases receive a harmonic signal consisting only of the repeated signal from the simulation with the normal magnet. Since we want to get the data which an attached piezo sensor would get, the deformation is extracted from the simulation model at the position where the piezo sensor would be attached on a real machine. This output therefore corresponds to the signal of the piezo sensor.
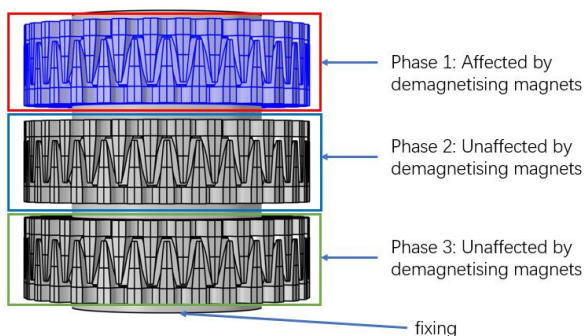
Figure 3: Transvere flux machine consisting of 3 phases, the faulty magnet is placed in phase 1

The resulting vibration signals were used as training data for a 1D convolutional neural network (CNN) for classification of the level of demagnetization of a single

magnet. Thus, the usage as a piezo element for condition monitoring during operation of the TFM was demonstrated in simulation. Besides condition monitoring, much more applications can be realized by using the same simulation model and modifying the simulations procedure or boundary conditions, e.g. Active Vibration Control (AVC) during operation or the detection and correction of production errors during manufacturing.

2.2 Thermal Data Acquisition

Temperature sensors within the rotor close to the magnets would deliver valuable data to set the parameters of thermal modelling accordingly without too many estimated thermal material or interface parameter assumptions. The sensors also serve for condition monitoring throughout the lifetime. Also, of interest are heat flux sensors on the stator teeth facing the rotor to gather data of the heat exchange between these parts. Heat flux sensor integration is not investigated any further in this research.

By placing the sensor as close as possible to the magnets, the actual temperature can be determined. This enables various possibilities.

For the operating of the machine, the measured temperature can be used for condition monitoring. Here, possible damages of the magnets in form of demagnetization, which are caused by an overheating, can be avoided. In addition, due to the fact that the temperature affects the electromagnetic properties of the magnets and therefor the behavior of the EM, it allows to reduce the necessary thermal safety factors of the EM, compared to thermal modeling of the magnets with a bigger inaccuracy.

For modelling the temperature behavior of an EM, the measurements during operation over the lifetime can be fed back into the development process to validate the thermal simulation and adjust the parameters of the model. In combination with the piezo element mentioned above, the condition monitoring can be further improved. Each senor benefits from the available data of the other sensor. When looking at the event of demagnetization in operation and the detection of it, this becomes more obvious.

If the condition monitoring by the piezo element detects demagnetization, the temperature measurements can be used to determine the operating point which caused the overheating and therefore adjust the operation of the EM in the future.

The temperature sensor profits from the piezo element by comparing the theoretical temperature for demagnetization with the measured values and the parallel condition monitoring for demagnetization.

The challenge for integrating a sensor into the rotor, is the need for a contactless power supply and data transmission. This is mandatory, because any physical connection cause uneconomic maintenance.

In order to supply the sensor with energy, a wireless power transmission (WPT) was implemented. This has a 1p2p topology, so that it is overvoltage-resistant in the case of open-circuit operation. The secondary coil is mounted on the outer surface of the TFMs rotor and consists of the Würth 760308101107. The primary coil is mounted statically and consists of the Würth 760308103202. A Royer Converter produces the 85 kHz alternating current to supply the WPT. The coil system is designed to be compact so that it can be used on different sized rotors. Therefore, the coils are much smaller than the outer surface. This means that the secondary coil on the outrunner always rotates out of the field of the primary coil. Thus, the power transmission is interrupted. The energy that is transmitted in the short time is stored temporarily via a super capacitor.

The temperature sensor is the digital TMP117 with I^2C interface, which is controlled by a NINA-W102. The NINA consists of an ESP32 and a Bluetooth Low Energy unit. This is used to send the measured data contactless from the rotor to the measuring station. Furthermore, the NINA-W102 has an energy-saving mode, which reduces the consumption of the controller sensor unit from $P_m = 188$ mW while measuring to $P_{sl} = 7$ mW in sleep mode. This allows for a reduction in power consumption in the time when the super capacitor has not stored enough energy. A measurement cycle consists of the measurement and a time-varying sleep portion t_{sl}. For the measurement, a measurement time of at least $t_m = 1$ s is required to establish the bluetooth connection, measure the temperature and sending the data to the measurement station. This results in the average power:

$$P_{average} = \frac{P_m\, t_m + P_{sl} t_{sl}}{t_m + t_{sl}}$$

In order to validate the system, a test carrier was built in a rapid prototyping process that replicate the rotor of the TFM and is driven by a stepper motor. A gearbox made it possible to achieve speeds of 2,400 rpm and a step size of $0.05°$.

In order to investigate whether the WPT section provides sufficient energy for the controller sensor unit, it was replaced with a resistor that corresponds to the consumption of the sensor and controller. This showed that the system provides a continuous power of 85 mW at different speeds. From the average measurement cycle consumption, it was found out that measurements can be taken every 2.18 s. This was confirmed by the operation of the entire system. From a measurement interval of more than 2.5 s at a minimum speed of 50 rpm, the system is capable of continuous operation.

3   Structural Optimization

Other areas which have great potential for improving the reliability and performance of TFMs are structural aspects in development. Additive manufacturing processes such as selective laser melting (SLM) promise completely new possibilities for the design of soft magnetic components for EMs. These processes allow the direct production of parts without the restrictions of conventional manufacturing processes such as casting or milling. They offer a high degree of design freedom in shaping, which can be used, for example, to incorporate slot structures for targeted loss minimization and improvement of the direct drive, as well as to realize lightweight component designs. One of the main sources for losses are eddy current losses in the soft magnetic components. These can be reduced by using material alloys with low electrical conductivity such as FeSi, by integrating insulation layers, e.g. in the form of air slots or by insulating material, or by a combination of both [9]. For the considerations here, air slots are used to reduce eddy current losses. The geometric freedom allows a large number of slot arrangements, two of which were selected and analyzed by simulation. These variants are a further development of the slot arrangements from [10], where the stator was slotted exclusively from the inside. This resulted in a reduction of eddy currents, but a relatively short current path for the eddy currents due to the necessary connecting bar above the slots. It is therefore necessary to extend this eddy current path due to the lower resistivity of the Fe material with 0.1 µΩm compared to the FeSi6.7 material with 0.85 µΩm [11]. As shown in **Figure 4**, this is achieved by slitting alternately from the outside and from the inside. In addition, two different orientations of the slots were analyzed. In arrangement 1 (Figure 4 left) the slots are offset from the center of the pole, whereas in arrangement 2 (Figure 4 right) the slots are aligned towards the center of the pole or between the poles. Both arrangements have eight slots per pole pair with a thickness of 170 µm. The investigations of these new arrangements were carried out according to [9]. For the operating point, the currents $i_d = 0$ A and $i_q = 6$ A are induced at a constant speed of $n_N = 1100$ rpm and field-oriented control. In addition, the arrangement of [9] with the material Fe used here and identical slot parameters was investigated to evaluate the results.
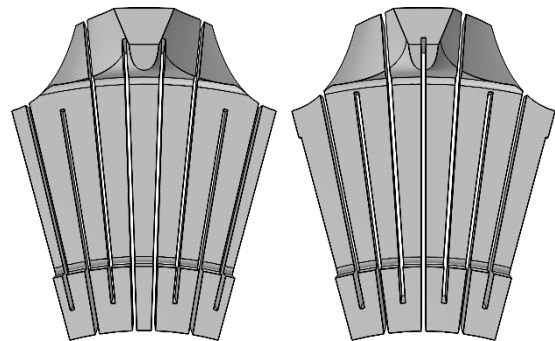
Figure 4: Analyzed slot arrangement 1 on the left and arrangement 2 on the right

The efficiency,

$$\eta = \frac{P_{\text{mech}}}{P_{\text{Cu}} + P_{\text{ec}} + P_{\text{mech}}}$$

is used as a criterion for the effectiveness of the new arrangements. This is based on the identical copper losses of $P_{\text{Cu}} = 9.93\,\text{W}$ for all arrangements, as well as the respective eddy current losses P_{ec} in the stator and the mechanical power P_{mech}. This resulted in an efficiency of $\eta = 26.2\,\%$ for the operating point considered of the initial design. By changing the slot arrangement, the efficiency could be increased to $\eta = 38.3\,\%$ for arrangement 1, or $\eta = 43.0\,\%$. for arrangement 2. However, it should be noted that the focus of the results here is to observe the effectiveness of different slot arrangements on eddy current losses. The FeSi materials used in the construction of electrical machines, such as FeSi6.7, have higher resistivities as described above, which would significantly improve efficiencies, but the brittleness of these materials presents greater processing challenges.

The basic manufacturing parameters and the proof of concept for loss reduction by implementing slots has already been shown in [10]. Kresse et al. identified a set of parameters for producing pure iron samples with a density of 7.83 g/cm³ (99.4 % relative density) but there was a trade-off in maximum bulk density and slot quality. Due to the electrically insulating function of the slots, a continuous separation is necessary. For this recent study the parameter sets have been divided into a core and shell (= slot surface) structure for further optimization. Based on previous additive manufacturing parameter studies various surface parameters have been tested. **Figure 5** shows a comparison of 200 and 250 µm laser track distances produced with those parameters. The samples were produced using a TruPrint1000 Multilaser, Trumpf SE + Co. KG, Germany and pure iron powder 99.9 %, particle
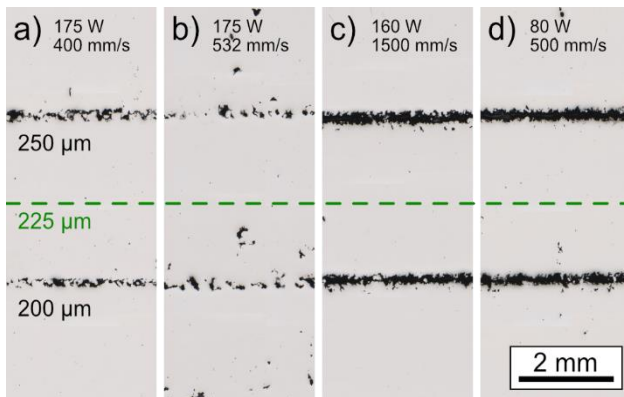
Figure 5: Comparison of slot qualities caused by different shell parameters. Constant core parameter of laser power $P_L = 175\,\text{W}$, scan velocity $vs = 400\,\text{mm/s}$, hatch distance $h = 90\,\mu\text{m}$. a) shell parameter = core parameter; b) increased scan velocity by 33 %, 175 W, 532 mm/s; c) support structure parameter 160 W, 1500 mm/s; d) surface parameter 80 W, 500 mm/s. Optical microscopy images.

size distribution +25/-70 µm ($D10 = 26\,\mu\text{m}$, $D50 = 41\,\mu\text{m}$, $D90 = 60\,\mu\text{m}$) from NANOVAL GmbH & Co. KG, Germany.

To overcome the statistical issue of a single cross section, CT scans of the produced geometries were carried out which allow for detail insights into part and slot quality (see **Figure 6**).
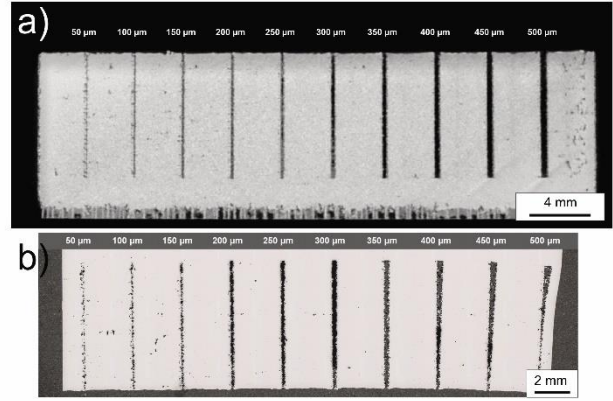
Figure 6: a) Cross-section of a CT scan of the process optimization to improve slot quality. b) Optical microscopy images of the same cut and polished specimen.

It is essential to ensure consistency between the simulated and the additively manufactured geometry of the specimen. Therefore, the relationship between the manufactured CAD model and the actual generated slot width was investigated. The preferable processing of additively manufactured slotted parts is done by creating a CAD model for printing with a slot width of 225 µm. By using the parameter d) from Figure 5 (80 W, 500 mm/s) the actual slot width is found to be approx. 170 µm.
The corresponding CAD model for simulations must therefore be designed with a slot width of 170 µm.

The difference between the track distance of the laser and the actual slot width is caused by the laser-parameter dependent diameter of the melt pool in additive manufacturing.

In addition to slot structures to reduce eddy current losses, the new geometric freedom promises to integrate cooling into the EM directly at the loss sources. This targeted cooling at the emerging hotspots can result in increased performance without risk of thermal damage to the EM. In this work, cooling channels leading through the stator next to the winding as well as through the individual stator teeth are simulatively analyzed and optimized. The average temperature of the passively cooled geometry reached 178.5 °C when thermal equilibrium was reached. Therefore, a machine with passive cooling cannot be run in continuous operation in the given load case. Compared to the passively cooled geometry, the average temperature across the stator with active cooling through the channels was reduced to 33.7 °C. The geometry of the cooling channels was then optimized to further reduce the

temperature. By incorporating these cooling channels into the stators and therefore changing the geometry, the electro-magnetic behavior is inherently altered. A larger cooling channel improves the heat dissipation, but in turn reduces the amount of flux-carrying material. Less flux-carrying material increases saturation effects in the stator and therefore decreases the efficiency. To take this into account during the optimization, a trade-off between large channels to reduce the temperature and small channels to preserve the flux-carrying material was chosen as the objective function. The results of the parametric optimization are shown in **Figure 7**. Only points on or close to the pareto front are shown.
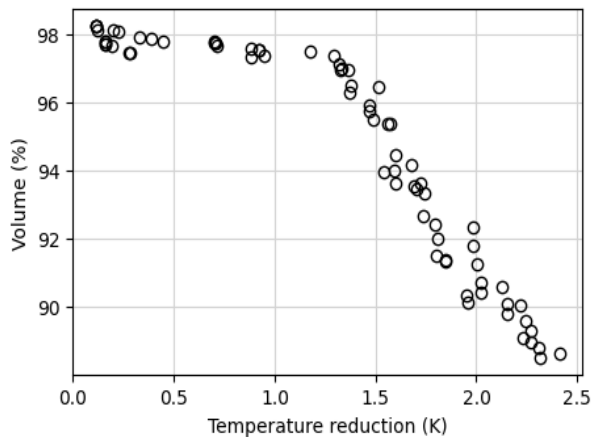
Figure 7: Pareto plot of cooling channel optimization

Each circle in the plot refers to a different geometry of the cooling channels. The temperature difference shown corresponds to the volumetric mean across the entire stator compared to the initial parameterization of the cooling channels. Therefore, the temperature difference appears to be small, although temperature peaks are reduced. Volumes ranging from 98 to 100 percent were omitted due to the resulting reduction in cooling channel diameters, which would be too small to manufacture. A distinct inflection point is visible in the Pareto front at a temperature reduction of approximately 1.3 K. This indicates that a larger temperature reduction results in a disproportionately high reduction of the flux-carrying material. Therefore, the design with the best compromise between volume reduction and temperature reduction can be found in the vicinity of the inflection point, at a volume reduction of approximately 2.5 %. As mentioned above, this change in geometry alters the electromagnetic behavior and therefore the heat losses and efficiency of the machine. The two-way coupling between the thermal and electromagnetic domains is an open topic for future work.

4   Summary & Outlook

This paper demonstrated different measures which could be used over the full product life cycle for improving the product properties of the TFM. It was shown that during operation piezo sensors and temperature sensors can be used for condition monitoring and performance enhancements by pushing the TFM closer to its limits. The free arrangement of slots through additive manufacturing in production can reduce eddy current losses. Incorporating cooling channels into the design can further increase the performance. Moreover, the settings of the laser for additive manufacturing where optimized.

All of the measures described above can when considered separately improve the TFM and make a usage in real applications more likely. A combination of the measures can improve the product properties even further. For example, a combination of the improved cooling performance and the constant measurement of the temperature inside the motor can be used for an adaptive performance increase of the TFM. Moreover, the data of the sensors can be used to learn more about how the TFM is used in different applications and uncover unused potentials.

However, so far only some combinations of the measures have been analyzed, specifically the structural improvements or the sensor/actuator integration, but without incorporating all of them into one unified machine. There are target conflicts to be expected, e.g. the optimization of the structure of the TFM could make locations inaccessible where the application of the sensors and actuators would be best suited. Moreover, the measures have been developed without explicitly checking for durability of the TFM. Therefore, the next steps are to combine the individual measures and investigate them in a TFM under real loads and environmental conditions.

5   Literature

[1]   N. Parspour, "Novel drive for use in electrical vehicles," 2005 IEEE 61st Vehicular Technology Conference, Stockholm, Sweden, 2005, pp. 2930-2933 Vol. 5, https://doi.org/10.1109/VETECS.2005.1543883.

[2]   P. Seibold, F. Schuller, M. Beez and N. Parspour, "Design and measurement of a laminated permanent magnet excited transverse flux machine for electrical vehicles," 2014 4th International Electric Drives Production Conference (EDPC), Nuremberg, Germany, 2014, pp. 1-6, https://doi.org/10.1109/EDPC.2014.6984411.

[3]   A. Albers, N. Bursac, E. Wintergerst, „Produktgenerationsentwicklung – Bedeutung und Herausforderungen aus einer entwicklungsmethodischen Perspektive", 2015, Stuttgarter Symposium Für Produktentwicklung 2015, Stuttgart, Germany

[4]   J. Gausemeier, U. Lindemann, G. Reinhart, H. Wiendahl, „Kooperatives Produktengineering - Ein neues Selbstverständnis des ingenieurmäßigen Wirkens", 2000 Verlagsschriftenreihe des Heinz Nixdorf Instituts, Paderborn, Band 79, Heinz

Nixdorf Institut, Universität Paderborn, ISBN 3-931466-78-7

[5] T. Sakao and A. K. Nordholm, "Requirements for a Product Lifecycle Management System Using Internet of Things and Big Data Analytics for Product-as-a-Service", 2021, Front. Sustain., 2 (735550), https://doi.org/10.3389/frsus.2021.735550

[6] C. Rivera, J. Poza, G. Ugaldem, G. Almandoz, "A Requirement Engineering Framework for Electric Motors Development", 2018, Applied Sciences, 8(12), 2391. MDPI AG, http://dx.doi.org/10.3390/app8122391

[7] G. Lei, J. Zhu, Y. Guo, "Multidisciplinary Design Optimization Methods for Electrical Machines and Drive Systems", 2016, Power Systems. Springer, Berlin, Heidelberg., https://doi.org/10.1007/978-3-662-49271-0

[8] M. Henger, "Zur Betriebsfestigkeit elektrischer Maschinen in Elektro- und Hybridfahrzeugen", 2012, Springer-Verlag, https://doi.org/10.1007/978-3-658-00707-2.

[9] D. Goll, D. Schuller, G. Martinek, T. Kunert, J. Schurr, C. Sinz,T. Schubert, T. Bernthaler, H. Riegel, and G. Schneider, "Additivemanufacturing of soft magnetic materials and components," Additive Manufacturing, vol. 27, pp. 428–439, 2019.

[0] M. Schmid, J. Terfurth, K. Kaiser and N. Parspour, "Electromagnetic Design of Electrical Machines - New Potentials of Additive Manufacturing with the Example of the Transverse Flux Machine," 2022 International Conference on Electrical Machines (ICEM), Valencia, Spain, 2022, pp. 1491-1497, https://doi.org/10.1109/ICEM51905.2022.9910628.

[11] T. Kresse, J. Schurr, M. Lanz, T. Kunert, M. Schmid, N. Parspour, G. Schneider, D. Goll, "Additively Manufactured Transverse Flux Machine Components with Integrated Slits for Loss Reduction", 2022 Metals 12 (11), S. 1875, https://doi.org/10.3390/met12111875.

6   Acknowledgements

www.kit.edu